ISSN 1392 - 1207. MECHANIKA. 2011. 17(5): 503-509

Dynamic characterization and stability analysis of hydrodynamic journal bearing using the FEM

Dj. Boukhelef*, A. Bounif, Dj. Amar Bouzid*****
**Department of Material Engineering, University of Medea, Algeria, E-mail: djboukhelef@yahoo.fr*
***University of Sciences and Technology, Oran, Algeria, E-mail: bounif@univ-ust.dz*
****Department of Material Engineering, University of Medea, Algeria, E-mail: d_amarbouzid@yahoo.fr*

crossref http://dx.doi.org/10.5755/j01.mech.17.5.727

1. Introduction

Analytically, lubrication which belongs to field problems is governed by Reynolds equation. The solution of this well-known equation provides the distribution of the pressure field generated in the fluid during working. This, allows us to determine both static and dynamic characteristics in solving Reynolds equation numerically using the variational principle [1-3].

Many Finite Element and Finite Difference methods along with analytical and experimental procedures have been successfully used in the study of hydrodynamic lubrication. Most papers focused on the computation of stiffness and dumping coefficients. Indeed, Woodcock and Holmes [4] and Glienicke [5] used experimental procedure in order to establish dynamic coefficients. Rao [6] employed analytical approach to predict past whirl orbits and dynamic coefficients as well. In addition to the above work, other authors used the Finite Differences method to solve the problem.

On one hand, Subiah et al [7] using the FD method, computed dynamic coefficients. On the other hand, EDF and LMS, developed a computer code EDYOS [8] to determine static and dynamic performance along with stability prediction.

Stability is also a fundamental criterion in journal bearing analysis. For more details about stability analyses, the reader is referred to references [9-15].

By modelling the fluid film acting as a lubricant between the journal and bearing, by means of Finite Elements, this paper has been organised as fellows. Firstly, stiffness and damping coefficients have been numerically established and compared to those of other methods encompassing, Finite differences results and experimental data. Secondly, a limited parametric study in which the effect of rotor dimensions, as well as relative eccentricity on the stability of a rotating machine have also been examined.

2. Basic lubrication theory

The lubrication analysis is an important problem in tribology. It deals with the contact study of two surfaces in relative movements. These areas are separated by a fluid film, which plays the role of lubricant. In this study let us consider a circular plain journal bearing represented by Fig. 1.

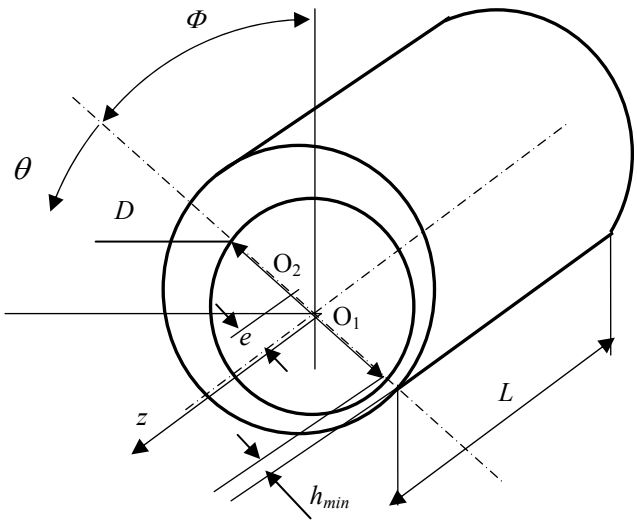

L - journal bearing length

$D = 2R$ - shaft diameter

e - eccentricity

Φ - attitude angle

θ - circumferential coordinate

Fig. 1 Geometry of plain journal bearing

2.1. Reynolds equation

The differential equation governing the pressure generation in hydrodynamic lubrication is due to Reynolds (1886) and is derived from conservation equations of mass and momentum. The general Reynolds equation of lubrication [16] is given as

$$\frac{1}{R^2}\frac{\partial}{\partial\theta}\left(\frac{h^3}{12\mu}\frac{\partial P}{\partial\theta}\right)+\frac{\partial}{\partial z}\left(\frac{h^3}{12\mu}\frac{\partial P}{\partial z}\right)=\frac{1}{2}\omega\frac{\partial h}{\partial\theta}h+\frac{\partial h}{\partial t} \quad (1)$$

where P is the pressure filed in lubricant, R is shaft radius, h is film fluid thickness, ω is the angular velocity of the shaft, μ is the viscosity of lubricant and $\partial h/\partial t$ is the

squeeze film term taken into account in dynamic case especially to calculate dynamic coefficients.

In the static case the rotation axis of the shaft is constant and the squeeze film term vanishes. The boundary conditions associated to the pressure distribution, so-called Reynolds conditions, are

$$\left.\begin{aligned} &P(\theta=0,\ z)\ =\ 0 \\ &P(\theta,z=0)\ =\ 0 \\ &P(\theta,\ z)\ =\ 0 \qquad \text{for}\ \ \theta_s \le \theta < 2\pi \\ &\frac{\partial P}{\partial \theta}(\theta=\theta_s,\ z) = \frac{\partial P}{\partial z}(\theta=\theta_s,\ z)=0 \end{aligned}\right\} \tag{2}$$

where θ_s is failure angle in fluid film.

3. Dynamic analysis

For dynamic operating state it is important to take the flexibility of bearing lubricant films into account by evaluating effective stiffness and damping coefficients. These parameters have a significant effect on system critical speeds, on forced response and on system stability. This may be done by considering the changes in both carrying pressure ΔP and film thickness Δh due to change of the applied loads [7]. These changes may be obtained from Taylor series as follows:

$$\Delta P = P_x \Delta x + P_y \Delta y + P_{\dot{x}} \Delta \dot{x} + P_{\dot{y}} \Delta \dot{y} \tag{3a}$$

$$\Delta h = \Delta x\ cos\,\theta + \Delta y\ sin\,\theta \tag{3b}$$

where $\Delta x, \Delta y, \Delta \dot{x}$ and $\Delta \dot{y}$ represent the changes on displacement and velocities along x and y directions respectively.

Indeed, for small perturbations around the static position of the journal, the pressure and the thickness of the fluid film may be expressed, by neglecting higher order terms, as follows:

$$\Delta P = P_0 + P_x \Delta x + P_y \Delta y + P_{\dot{x}} \Delta \dot{x} + P_{\dot{y}} \Delta \dot{y} \tag{4a}$$

$$h\ =\ h_0 + \Delta x\, cos\theta + \Delta y\, sin\theta \tag{4b}$$

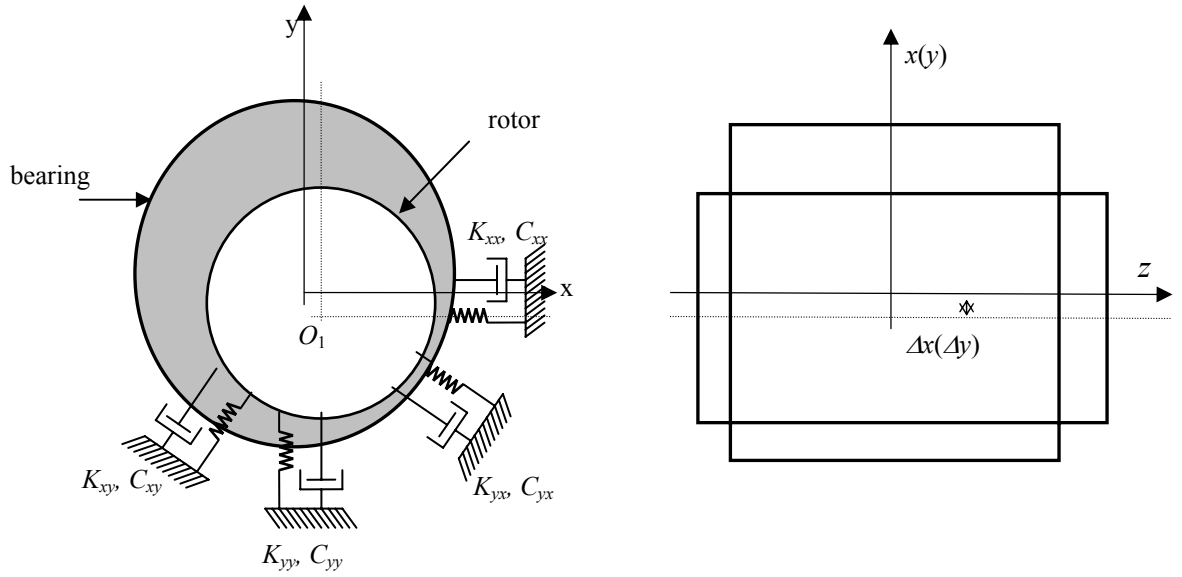

a b

Fig. 2 Dynamic operating system: a - dynamic modeling, b - dynamic displacements

Substituting Eqs. (4a) and (4b) into Reynolds Eq. (1) and arranging terms according to $\Delta x, \Delta y, \Delta \dot{x}$ *and* $\Delta \dot{y}$ respectively, one obtains the following equations [7]:

$$L\left(\bar{P}_0\right) = 12\pi \frac{\partial \bar{h}_0}{\partial \theta} \tag{5}$$

$$L\left(\bar{P}_x\right) = -12\pi\left(sin\theta + 3\frac{cos\theta}{\bar{h}_0}\frac{\partial \bar{h}_0}{\partial \theta}\right) - 3\bar{h}_0^3 \frac{\partial}{\partial \theta}\left(\frac{cos\theta}{\bar{h}_0}\right)\frac{\partial \bar{P}_0}{\partial \theta} \tag{6}$$

$$L\left(\bar{P}_y\right) = 12\pi\left(cos\theta - 3\frac{sin\theta}{\bar{h}_0}\frac{\partial \bar{h}_0}{\partial \theta}\right) - 3\bar{h}_0^3 \frac{\partial}{\partial \theta}\left(\frac{sin\theta}{\bar{h}_0}\right)\frac{\partial \bar{P}_0}{\partial \theta} \tag{7}$$

$$L\left(\bar{P}_{\dot{x}}\right) = 12 cos\theta \tag{8}$$

$$L\left(\bar{P}_{\dot{y}}\right) = 12 sin\theta \tag{9}$$

where $L(F)$ is an operator applied to a function F and defined by

$$L(F) = \frac{\partial}{\partial \theta}\left(\bar{h}_0^3 \frac{\partial F}{\partial \theta}\right) + \left(\frac{D}{L}\right)^2 \frac{\partial}{\partial \bar{z}}\left(\bar{h}_0^3 \frac{\partial F}{\partial \bar{z}}\right) \tag{10}$$

The dimensionless quantities are defined by:

$$\left.\begin{aligned} &\bar{h}_0 = \frac{h_0}{c}, \quad \bar{z} = \frac{2z}{L} \\ &P_0 = \mu N\left(\frac{R}{c}\right)^2 \bar{P}_0, \quad P_x, P_y = \mu \frac{N}{c}\left(\frac{R}{c}\right)^2 \bar{P}_x, \bar{P}_y, \\ &P_{\dot{x}}, P_{\dot{y}} = \frac{\mu}{c}\left(\frac{R}{c}\right)^2 \bar{P}_{\dot{x}}, \bar{P}_{\dot{x}} \end{aligned}\right\} \tag{11}$$

where, h_0 is film thickness, c is the clearance of journal bearing, μ is the fluid viscosity and N is the rotational speed, rpm.

4. Finite element modelling and Reynolds equation resolution

As far as accuracy in modelling is concerned it is always desirable to search for powerful numerical methods. The finite element method is among the robust methods applied in mechanical engineering. In the present work, this widely used method is employed to resolve the Reynolds equation in order to obtain bearing characteristics.

As the fluid film is extremely thin, it is possible to consider its developed form (Fig. 3, a) for numerical analysis purpose. Hence, the fluid film is discretized into a set of six-noded Finite Elements in both circumferential and axial directions (Fig. 3, b). This type of element has a quadratic field of pressure, and consequently it constitutes a well compromise between complexity and accuracy. The shape functions associated to this element (Fig. 3, c) are:

- at corner nodes 1, 2, and 3:

$$\left.\begin{aligned} N_1(\xi,\eta) &= (1-\xi-\eta)(1-2\xi-2\eta) \\ N_2(\xi,\eta) &= \xi(2\xi-1) \\ N_3(\xi,\eta) &= \eta(2\eta-1) \end{aligned}\right\} \quad (12a)$$

- at mid-side nodes 4, 5 and 6:

$$\left.\begin{aligned} N_4(\xi,\eta) &= 4\xi(1-\xi-\eta) \\ N_5(\xi,\eta) &= 4\xi\eta \\ N_6(\xi,\eta) &= 4\eta(1-\xi-\eta) \end{aligned}\right\} \quad (12b)$$

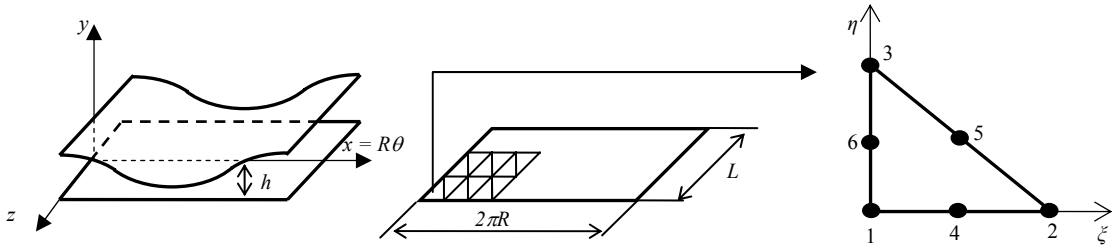

a b c

Fig. 3 Finite element modelling: a - developed journal bearing, b - F.E. Mech of fluid film, c - six nodded element

According to the variational principle, the variational form of Reynolds equation is given by [1]:

$$I(\bar{P}_x) = \frac{1}{2}\int_A \left\{ \bar{h}_0^3 \left(\frac{\partial \bar{P}_x}{\partial \theta} \right) + \left(\frac{D}{L} \right)^2 \bar{h}_0^3 \left(\frac{\partial \bar{P}_x}{\partial z} \right) + 2 f_x \bar{P}_x \right\} dA \quad (13a)$$

$$f_0 = 12\pi \frac{\partial \bar{h}_0}{\partial \theta} \quad (13b)$$

where A is the resolution of Reynolds equation in static case yields the pressure field in the film lubricant. The loading capacity components are given by

$$W_x = R\int_s P \sin\theta \, ds, \quad W_y = R\int_s P \cos\theta \, ds \quad (14)$$

The loading capacity W whose components are given by Eq. (14), can be put in a dimensionless form as

$$\bar{W} = \frac{W}{\mu L D N}\left(\frac{c}{R} \right)^2 \quad (15)$$

Sommerfield number which characterises the dimensionless load is written as

$$S = \frac{1}{\pi \bar{W}} \quad (16)$$

The equivalent variational forms of Eqs. (6) to (9) are respectively

$$I(\bar{P}_x) = \frac{1}{2}\int_A \left\{ \bar{h}_0^3 \left(\frac{\partial \bar{P}_x}{\partial \theta} \right) + \left(\frac{D}{L} \right)^2 \bar{h}_0^3 \left(\frac{\partial \bar{P}_x}{\partial z} \right) + 2 f_x \bar{P}_x \right\} dA \quad (17)$$

$$I(\bar{P}_y) = \frac{1}{2}\int_A \left\{ \bar{h}_0^3 \left(\frac{\partial \bar{P}_y}{\partial \theta} \right) + \left(\frac{D}{L} \right)^2 \bar{h}_0^3 \left(\frac{\partial \bar{P}_y}{\partial z} \right) + 2 f_y \bar{P}_y \right\} dA \quad (18)$$

$$I(\bar{P}_{\dot{x}}) = \frac{1}{2}\int_A \left\{ \bar{h}_0^3 \left(\frac{\partial \bar{P}_{\dot{x}}}{\partial \theta} \right) + \left(\frac{D}{L} \right)^2 \bar{h}_0^3 \left(\frac{\partial \bar{P}_{\dot{x}}}{\partial z} \right) + 2 f_{\dot{x}} \bar{P}_{\dot{x}} \right\} dA \quad (19)$$

$$I(\bar{P}_{\dot{y}}) = \frac{1}{2}\int_A \left\{ \bar{h}_0^3 \left(\frac{\partial \bar{P}_{\dot{y}}}{\partial \theta} \right) + \left(\frac{D}{L} \right)^2 \bar{h}_0^3 \left(\frac{\partial \bar{P}_{\dot{y}}}{\partial z} \right) + 2 f_{\dot{y}} \bar{P}_{\dot{y}} \right\} dA \quad (20)$$

with

$$f_x = -12\pi \left(\sin\theta + 3\frac{\cos\theta}{\bar{h}_0}\frac{\partial \bar{h}_0}{\partial \theta} \right) - 3\bar{h}_0^3 \frac{\partial}{\partial \theta}\left(\frac{\cos\theta}{\bar{h}_0} \right)\frac{\partial \bar{P}_0}{\partial \theta} \quad (21)$$

$$f_y = 12\pi \left(\cos\theta + 3\frac{\sin\theta}{\bar{h}_0}\frac{\partial \bar{h}_0}{\partial \theta} \right) - 3\bar{h}_0^3 \frac{\partial}{\partial \theta}\left(\frac{\sin\theta}{\bar{h}_0} \right)\frac{\partial \bar{P}_0}{\partial \theta} \quad (22)$$

$$f_{\dot{x}} = 12\cos\theta \quad (23)$$

$$f_{\dot{y}} = 12\sin\theta \quad (24)$$

Eq. (5), which is simply Eq. (1) for the static case, must be resolved primarily according to boundary conditions (2). Then by solving Eqs. (6) to (9), it becomes easy to obtain pressures $\bar{P}_x$, $\bar{P}_y$, $\bar{P}_{\dot{x}}$ and $\bar{P}_{\dot{y}}$ respectively and then deduce bearing characteristics.

5. Dynamic characteristics

The bearing features to be taken into account in dynamic analysis of rotors are the eight lubricant film stiffness and damping coefficients. These quantities may be expressed as follows [16]:

- stiffness coefficients:

$$\left.\begin{aligned} K_{xx} &= \int_s P_x \cos\theta \, ds, \qquad K_{xy} = \int_s P_x \sin\theta \, ds \\ K_{yx} &= \int_s P_y \cos\theta \, ds, \qquad K_{yy} = \int_s P_y \sin\theta \, ds \end{aligned}\right\} \tag{25}$$

- damping coefficients:

$$\left.\begin{aligned} C_{xx} &= \int_s P_{\dot{x}} \cos\theta \, ds, \qquad C_{xy} = \int_s P_{\dot{x}} \sin\theta \, ds \\ C_{yx} &= \int_s P_{\dot{y}} \cos\theta \, ds, \qquad C_{yy} = \int_s P_{\dot{y}} \sin\theta \, ds \end{aligned}\right\} \tag{26}$$

In dimensionless forms dynamic coefficients are given as:

$$\bar{K}_{ij} = \frac{CK_{ij}}{\mu NDL\left(\frac{R}{C}\right)^2}, \quad \bar{C}_{ij} = \frac{C\omega\, C_{ij}}{\mu NDL\left(\frac{R}{C}\right)^2}. \tag{27}$$

6. Validation of the finite element results

In order to verify the validity of the finite element results presented in this work, the comparison was made with another numerical method carried out by (EDF and LMS) [8], and with experimental work achieved by (Woodcock and Holmes) [4]. Hence, EDF used Finite Difference method to analyse dynamic performance of finite journal bearing.

Fig. 4 show the evolution of stiffness coefficients $\bar{K}_{xx}$, $\bar{K}_{xy}$, $\bar{K}_{yx}$, $\bar{K}_{yy}$ against the eccentricity ratio for a journal bearing of L/D = 0.5, on one hand ad makes comparison between the results of the three types of analysis on the other hand.

Three important points can be drawn from the examination of Fig. 4. Firstly, while the cross-coupling $\bar{K}_{yx}$ presents an excellent agreement between the three types of analyses, a quite good accordance is observed for the three other stiffness coefficients in the range of eccentricity ratio between 0.1 and 0.5. Secondly, FE results slightly underestimate stiffness coefficient beyond the value of eccentricity ratio equal to 0.5.

In addition to the examination of stiffness coefficient it is convenient and useful to consider damping coefficient for comparison. Hence, the damping coefficients $\bar{C}_{xx}$, $\bar{C}_{xy}$, $\bar{C}_{yx}$, $\bar{C}_{yy}$ corresponding to a journal bearing of L/D = 0.5, are plotted against the eccentricity ratio in Fig. 5.

As it can be seen from this Figure, the agreement between the Finite Elements values of damping coefficient and those of the FD method is quite good for almost the entire range of eccentricity ratio. However, a slight discrepancy is observed between results of the present work and those of the experimental procedure.

It can be concluded from the accuracy of the above comparisons that the current analyses are convenient for parametric study that can present computational results which might be used in both practical and academic purposes.

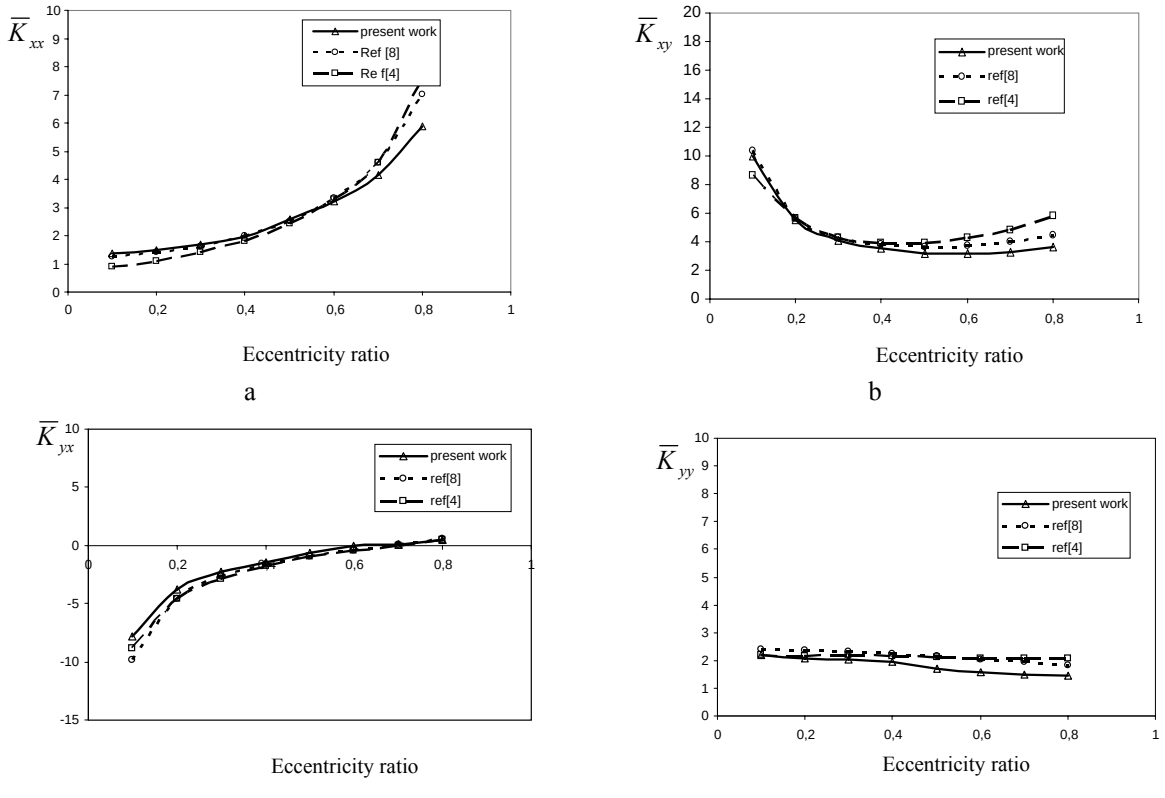

Fig. 4 Variation of stiffness coefficients with eccentricity ratio: a - $\bar{K}_{xx}$, b - $\bar{K}_{xy}$, c - $\bar{K}_{yx}$, d - $\bar{K}_{yy}$

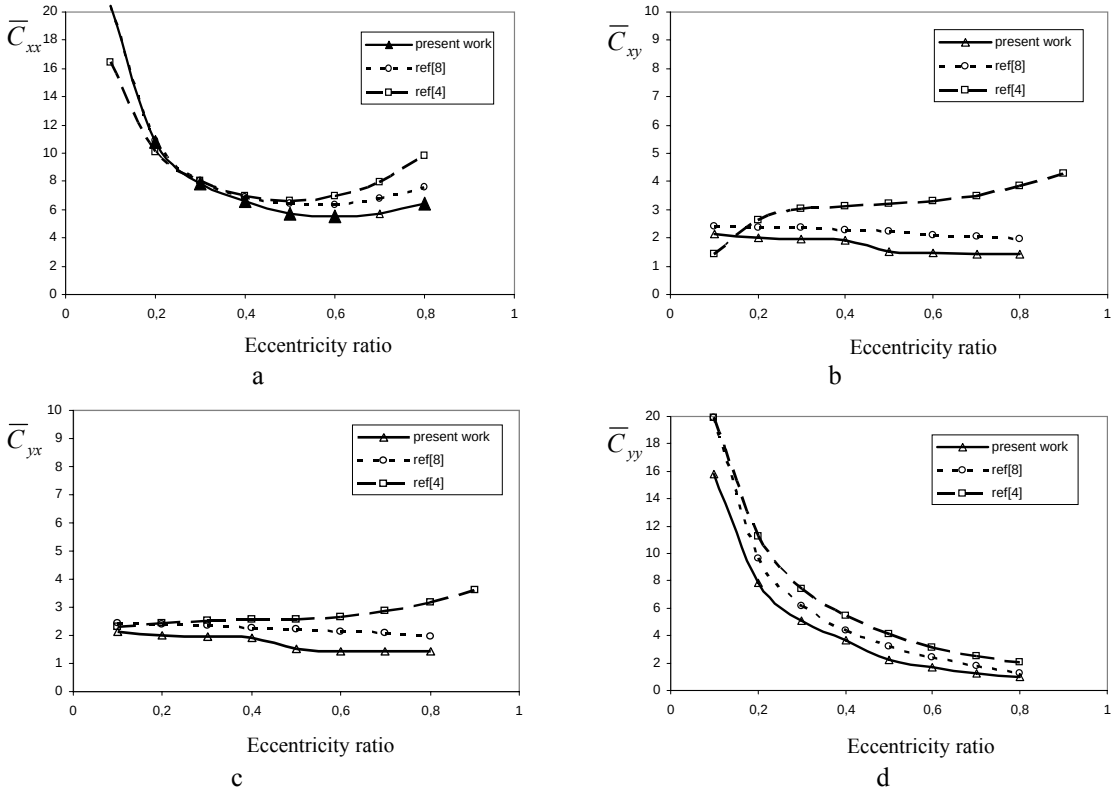

Fig. 5 Variation of damping coefficients with eccentricity ratio: a - $\overline{C}_{xx}$, b - $\overline{C}_{xy}$, c - $\overline{C}_{yx}$, d - $\overline{C}_{yy}$

7. Parametric study

In addition to their dependence on the eccentricity ratio, the stiffness ad damping coefficients depend on the bearing ratio *L/D* as well.

In this section a limited parametric study has been

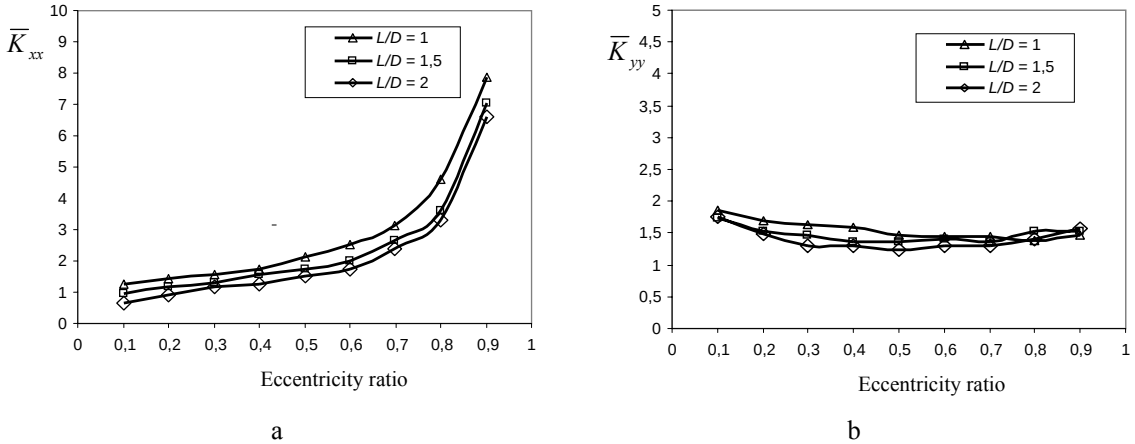

Fig. 6 Stiffness coefficients for different values of *L/D*: a - $\overline{K}_{xx}$, b - $\overline{K}_{yy}$

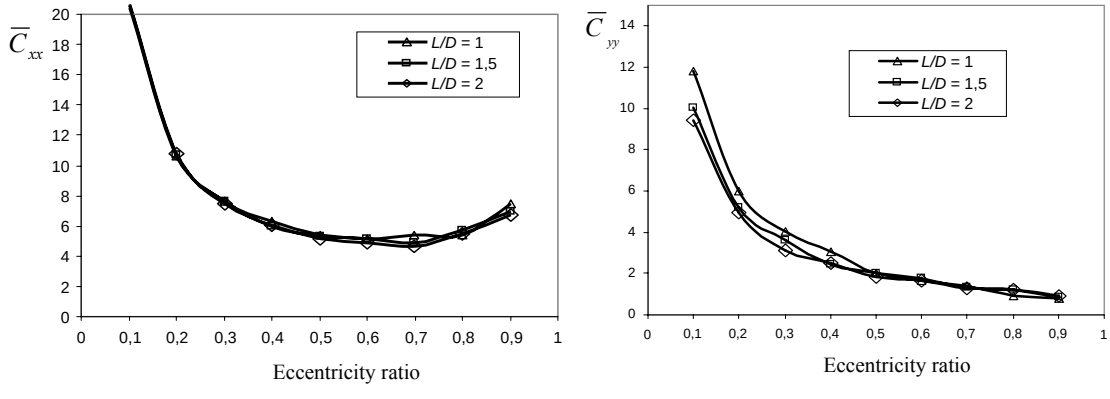

Fig. 7 Damping coefficients for different values of *L/D*: a - $\overline{C}_{xx}$, b - $\overline{C}_{yy}$

undertaken to see the influence of *L/D* on the variation of stiffness coefficients $\overline{K}_{xx}$, $\overline{K}_{yy}$ and damping coefficients $\overline{C}_{xx}$, $\overline{C}_{yy}$ with the eccentricity ratio.

Hence, three bearing ratios were chosen namely: *L/D* = 1, *L/D* = 1.5 and *L/D* = 2, in order to represent a wide range of engineering applications. Fig. 6, shows the effect of *L/D* on the stiffness coefficients $\overline{K}_{xx}$ and $\overline{K}_{yy}$, whereas Fig. 7 illustrates the effect of the same parameter on the damping coefficients $\overline{C}_{xx}$ and $\overline{C}_{yy}$. As it can be seen from both Figures, there is practically no influence of *L/D* on stiffness and damping coefficients for almost the entire range of the eccentricity ratio. However, a slight effect of *L/D* on the coefficient $\overline{C}_{yy}$ is observed for the small values of the eccentricity ratio in Fig. 7, b.

8. Stability analysis

We consider in this section a symmetric and rigid rotor of mass 2*M* carried by two identical journal bearings. The linear system governing its behaviour is given by

$$M\begin{Bmatrix}\ddot{x}\\ \ddot{y}\end{Bmatrix}+\left|K_{ij}\right|\begin{Bmatrix}x\\ y\end{Bmatrix}+\left|C_{ij}\right|\begin{Bmatrix}\dot{x}\\ \dot{y}\end{Bmatrix}=0 \tag{28}$$

where *x* and *y* are the displacement components of the shaft centre starting from static equilibrium position.

According to Routh-Hurwitz criterion [11, 16], the whirl frequency $\overline{\omega}_s$ and the critical mass $\overline{M}_c$ are expressed in terms of dynamic coefficients by the following equations:

$$\overline{\omega}_s^2=\frac{\left(\overline{K}_{xx}-\overline{K}_{eq}\right)\left(\overline{K}_{yy}-\overline{K}_{eq}\right)-\overline{K}_{xy}\overline{K}_{yx}}{\overline{C}_{xx}\overline{C}_{yy}-\overline{C}_{xy}\overline{C}_{yx}} \tag{29}$$

$$\overline{M}_c=\frac{\overline{K}_{eq}}{\overline{\omega}_s^2} \tag{30}$$

where

$$\overline{K}_{eq}=\frac{\overline{K}_{xx}\overline{C}_{yy}+\overline{K}_{yy}\overline{C}_{xx}-\overline{K}_{xy}\overline{C}_{yx}-\overline{K}_{yx}\overline{C}_{xy}}{\overline{C}_{xx}+\overline{C}_{yy}} \tag{31}$$

In order to have a wide sight, it has been judged useful to consider four slenderness ratios namely *L/D* = 05, *L/D* = 1, *L/D* = 1.5 and *L/D* = 2.

Indeed, Fig. 8 illustrates the evolution of the critical mass with the increasing Sommerfield number for the considered *L/D* values.

On the light of a close examination in this Figure, three important points can be drawn. Firstly, we notice that the stability is secured for higher eccentricities (> 0.75). This means for lower values for Sommerfiled number. Secondly, it is clearly seen that, the larger Sommerfiled number becomes, the smaller the critical mass gets for all slenderness ratios considered. Thirdly, for low eccentricities (high values of Sommerfield number), Reynolds boundary conditions are no longer valid. Consequently, the journal bearing becomes instable.

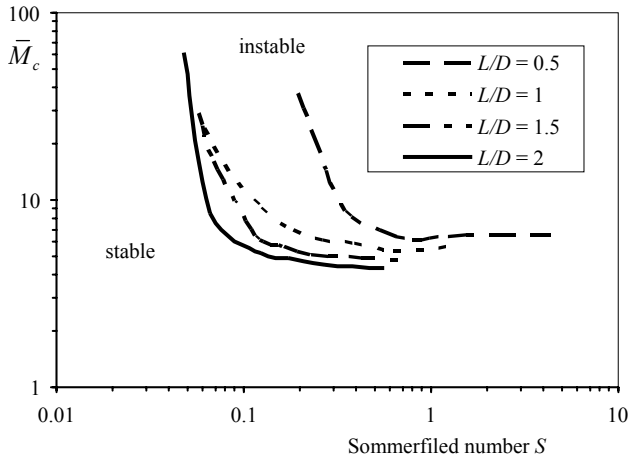

Fig. 8 Variation of $\overline{M}_c$ with *S*

9. Conclusions

As far as accurate computation of dynamic coefficients is concerned, the Finite Element method is the natural choice for the dynamic analysis of journal bearings. In the present paper, this versatile and powerful method has been applied to compute bearing characteristics, especially stiffness and dynamic coefficients.

After a brief presentation of lubrication theory, the different governing equations deduced from the discretization by finite elements were presented. Then, FE results were compared to another robust method, which is the FD approach, as well as with experimental data. Indeed, the evolution of stiffness as well as damping coefficients against the eccentricity ratio was thoroughly examined. The results of comparison were satisfactory. On the basis of that the numerical approach had showed its ability to predict accurate coefficients, a very limited parametric study involving the effect of slenderness ratio on the evolution of dynamic coefficients, has been undertaken. Results of the analysis were then discussed.

The presented problem of dynamic characterization of journal bearings using the FEM, has both a practical and theoretical significance. The practical significance is obvious and the theoretical significance is that the present computational results can be used to validate other numerical methods.

References

1. **Hubner, K.H.** 1975. The Finite Element Method Engineers, John Wiley and sons.
2. **Rao, S.S.** 1982. The Finite Element Method in Engineering. Pergamon press.
3. **Allaire, P.; Cnicholas, J.; Gunter, E.J.** 1977. Systems of finite elements for finite bearings, Journal of Lubrication Techn. Trans ASME: 187-197.
4. **Woodcock, J.S.; Holmes, R.** 1970. Determination and application of the dynamic proprieties of turbo-rotor bearing oil film. Proc. Inst. Mech engrs, vol 184(32): 111.
5. **Glienicke, J**. 1967. Experimental investigation of the stiffness and damping coefficients of turbine bearing and their application to instability prediction. Proc. Inst. Engs, vol 181 (3B): 116.
6. **Rao, T.V.L.N.; Biswas, S.; Hirani, H.; Athre, K.**

2000. An analytical approach to evaluate dynamic coefficients and nonlinear transient analysis of hydrodynamic journal bearing, Tribology Transactions 43(1): 109-115.
7. **Subiah, R.; Bhat, R.B.; Sankar, T.S**. 1985. Rotational stiffness and damping coefficients of fluid film in finite cylindrical bearing, ASLE 29: 414-422.
8. **EDF, LMS.** 2004. **(**France**),** Software EDYOS.
9. **Rho, B.H.; Kim, K.W.** 2002. A study of stability characteristics of actively controlled hydrodynamic journal bearings, JSME International Journal, serie C, Vol.45(1).
10. **Menh, N.C.** 2008. The influence of elastic base on stability of rotor-oil film bearing systems, Technische Mechanick, band 28, heft 3-4: 194-203.
11. **Swanson, E.** 2005. Fixed-geometry, hydrodynamic bearing with enhanced stability characteristics. Tribology Transactions 48: 82-92.
12. **Tuma, J.; Bilosova, A.; Simek, J.; Svoboda, R.** 2008. A simulation study of the rotor vibration in journal bearing, Engineering Mechanics 15(6): 461-470.
13. **Husben, G.B.; Rattan, S.S.; Mehta N.P**. 2007. Effect of L/D ratio on the performance of a four-lobe pressure dam bearing, Word Academy of Science, Engineering and Technology 32.
14. **Andres, S.L.; Santiago, O.** 2005. Identification of journal bearing force coefficients under high dynamic loading centred static operation, Tribology Transactions 43(9): 9-17.
15. **Jang, G.H.; Yoon, J.W.** 2003. Stability analysis of a hydrodynamic journal bearing with rotating herringbone grooves, Journal of Tribology 125(4): 291-300.
16. **Frene, J.; Nicolas, D.; Dgueurce, B.; Berthe, D.; Godet, M.** 1990. Lubrification hydrodynamique – paliers et butées. Eyrolles.

Dj. Boukhelef, A. Bounif, Dj. Amar Bouzid

HIDRODINAMINIŲ SLYDIMO GUOLIŲ DINAMINIS ĮVERTINIMAS IR STABILUMO ANALIZĖ TAIKANT BAIGTINIŲ ELEMENTŲ METODĄ

R e z i u m ė

Kadangi išsidėvėjimas yra vienas iš svarbiausių sukimosi mašinų pažeidimo tipų, reikia, o gal net privalu, nustatyti slydimo guolių charakteristikas, būtinas saugiam mašinų darbui. Tepalai, pavyzdžiui, skysčio plėvelė, reikalinga tam, kad būtų išvengta sukimosi mašinų rotoriaus ir statoriaus kontakto. Tokių mašinų darbo metu skystyje sukuriamas slėgis radialiniam krūviui išlyginti. Pagrindinis šio darbo tikslas – taikant baigtinių elementų metodą apriboti apskritiminių slydimo guolių dinamines charakteristikas. Taigi šis straipsnis remiasi skaitiniu Reynoldso lygties, išreiškiančios slėgio pasiskirstymą skysčio plėvelėje, sprendimu. BE rezultatai gerai sutapo su kitais gautais metodais rezultatais. Ribota parametrinė studija, naudojant dinaminių charakteristikų santykio (*L*/*D*) efektą, bus atlikta vėliau kartu su stabilumo analize.

Dj. Boukhelef, A. Bounif, Dj. Amar Bouzid

DYNAMIC CHARACTERIZATION AND STABILITY ANALYSIS OF HYDRODYNAMIC JOURNAL BEARING USING THE FEM

S u m m a r y

As wear is considered among one of the main weakness factors of rotating machines, it is becoming compulsory if not mandatory to determine the characteristics of journal bearings required to insure a successful working of the machine. Lubricants, such as fluid films are needed to avoid rotor and stator contact in rotating machines. During the working of the latter, a pressure is generated within the fluid in order to equilibrate the radial loads. The main objective of this paper is to address the dynamic characterization problem of finite circular journal bearings using the Finite Element Method. Hence, the present study is based on the numerical resolution of Reynolds equation which describes the pressure profiles in the fluid film. The comparison of FE results and those of other methods reported in the literature showed a good agreement. A limited parametric study involving the effect of slenderness ratio (*L*/*D*) on the dynamic properties, a long with a stability analysis have been carried out.

Received December 17, 2010
Accepted September 23, 2011